

文章编号: 1000-324X(2023)10-1169-07

DOI: 10.15541/jim20230058

## 燃烧合成氮化硅粉体的性能 一致性评价方法和应用

李宏华<sup>1</sup>, 东婉茹<sup>2</sup>, 王良<sup>1</sup>, 杨增朝<sup>1</sup>, 李江涛<sup>1</sup>

(1. 中国科学院理化技术研究所, 低温重点实验室, 北京 100190; 2. 齐鲁中科光物理与工程技术研究院, 济南 250000)

**摘要:** 陶瓷粉体的批次稳定性是陶瓷制品生产商最关心的核心指标, 却又长期无据可依。本研究以燃烧合成的氮化硅粉体为样本, 量化评价不同批次生产的氮化硅粉体的相似程度。首先构建了涵盖静态理化指标、动态流动性指标的粉体性能评价参数体系, 进而测试得到在该参数体系中氮化硅粉体的全部性能数据, 随后对所得性能数据分别采用余弦相似度法和欧氏距离法进行计算, 得到了粉体性能一致性评价数据。结果表明, 基于该参数体系的余弦相似度和欧氏距离均能反映批次粉体间的相似程度, 量化显示出不同批次粉体的差异, 两种方法的计算结果相互验证。对判定为不相似的粉体, 追溯工艺流程中的差异找到了控制氮化硅粉体一致性的关键环节—原料硅粉; 对判定为高度相似的粉体划分为同类, 为不同批次氮化硅粉体的类别划分提供了量化依据。该工作建立的“粉体性能一致性评价体系”为氮化硅粉体产品质量的批次稳定性(性能一致性)提供了有效的评价手段和量化依据。

**关键词:** 一致性评价; 氮化硅粉体; 余弦相似度; 欧氏距离

中图分类号: TQ174 文献标志码: A

## Consistency of Silicon Nitride Powders Produced by Combustion Synthesis: Evaluation and Application

LI Honghua<sup>1</sup>, DONG Wanru<sup>2</sup>, WANG Liang<sup>1</sup>, YANG Zengchao<sup>1</sup>, LI Jiangtao<sup>1</sup>

(1. Key Laboratory of Cryogenics, Technical Institute of Physics and Chemistry, Chinese Academy of Sciences, Beijing 100190, China; 2. Institute of Optical Physics and Engineering Technology, Qilu Zhongke, Jinan 250000, China)

**Abstract:** The batch stability of ceramic powders is a core indicator that manufacturers of ceramic products are most concerned about, yet has long been undocumented. In this study, the similarity of  $\text{Si}_3\text{N}_4$  powders produced in different batches was quantitatively evaluated by taking combustion-synthesized  $\text{Si}_3\text{N}_4$  powders as the sample. A system of powder performance evaluation parameters covering static physicochemical and dynamic flowability indices was firstly constructed. Then, all performance data of  $\text{Si}_3\text{N}_4$  powders in this parameter system were retested. Subsequently, the consistency evaluation data of  $\text{Si}_3\text{N}_4$  powders were obtained using the cosine similarity method and the Euclidean distance method. The results show that both methods based on this parameter system can reflect the similarity between

收稿日期: 2023-02-06; 收到修改稿日期: 2023-03-08; 网络出版日期: 2023-03-24

基金项目: 国家重点研发计划 (2022YFE0201200, 2017YFB0310303)

National Key R&D Program of China (2022YFE0201200, 2017YFB0310303)

作者简介: 李宏华(1994-), 女, 助理研究员. E-mail: lihonghua@mail.ipc.ac.cn

LI Honghua (1994-), female, lecturer. E-mail: lihonghua@mail.ipc.ac.cn

通信作者: 李江涛, 研究员. E-mail: lijiangtao@mail.ipc.ac.cn; 东婉茹, 助理工程师, E-mail: gntcdongwr@casiop.ac.cn

LI Jiangtao, professor. E-mail: lijiangtao@mail.ipc.ac.cn; DONG Wanru, junior engineer. E-mail: gntcdongwr@casiop.ac.cn

batches of powders and quantitatively show the differences between them. Calculation results of the two methods are mutually verified. For powders judged to be dissimilar, differences in the process were traced to find the key link in the consistency between the  $\text{Si}_3\text{N}_4$  powders and the raw silicon powders. For powders judged to be highly similar, they were classified as the same class. This study provides a quantitative basis for the classification of different batches of silicon nitride powders. The “Powder Consistency Evaluation System” established in this work presents an effective evaluation tool and quantitative basis for batch stability (performance consistency) of silicon nitride powder.

**Key words:** consistency evaluation; silicon nitride powders; cosine similarity; Euclidean distance

氮化硅( $\text{Si}_3\text{N}_4$ )陶瓷具有优良的耐磨、耐蚀、高热导、耐高温性能以及良好的抗热震性能,已广泛应用于航空航天、机械、电子电力、化工等领域<sup>[1-2]</sup>。随着氮化硅轴承球、氮化硅基板等氮化硅制品逐步应用于风力发电设备及新能源汽车等领域,氮化硅陶瓷的应用需求不断扩大,市场规模持续增长。氮化硅粉体作为生产氮化硅陶瓷的核心原料,其质量的稳定性、品质的一致性,对制品生产的工艺稳定和产品品质稳定起到决定性作用。

氮化硅粉体的主流生产工艺有氨解法和硅粉氮化法两种,以 UBE, Denka, Vesta, Stark 等几家企业为代表已经大规模使用。近年来,燃烧合成法制备氮化硅粉体以近零能耗、短流程、绿色制备的优势在氮化硅生产企业中异军突起,迅速扩张<sup>[3-4]</sup>。燃烧合成的氮化硅粉体在  $\alpha/\beta$  相含量、粒度分布、杂质含量等指标上已能做到和现有商用粉体相当或更优异的水平。但是,燃烧合成氮化硅粉体工艺作为一种新兴生产工艺,其工艺稳定性和产品品质的一致性尚未经过市场认证,企业自身对产品品质的把关评价就相当关键,需要建立起一套一致性评价体系来控制粉体的稳定性。

当前氮化硅粉体的一致性评价仍是行业内面临的共性难题。一方面,粉体性能指标模糊,常用的指标为高  $\alpha$  相含量(>93%, 质量分数),低氧含量(<1.5%, 质量分数),细粒度( $D_{50}=0.6\sim0.8 \mu\text{m}$ ),高纯度(Fe, Al, Ca< $100\times10^{-6}$ ),但满足上述指标的粉体烧结制品的性能却存在差异<sup>[5-6]</sup>,粉体性能指标的评定无据可依;另一方面,若从粉体应用效果角度进行评价,即用陶瓷制品性能作为评价粉体性能的评价依据,则存在评价周期长、受烧结工艺流程中意外因素、制品性能测试误差等影响性能数据的问题,难以分辨引起陶瓷产品性能波动的主要原因是否在于粉体原料。粉体产品质量的批次稳定性缺乏有效的评价手段和量化依据已成为亟需解决的问题。

本研究针对氮化硅粉体的一致性评价问题,参考颗粒标准体系<sup>[7]</sup>和粉体药物一致性评价方法<sup>[8-10]</sup>,

结合生产实际,以静态理化指标、动态流动性指标为主体构建了粉体性能评价参数体系,并将此参数体系应用于不同批次燃烧合成生产氮化硅粉体的性能评价中,对所得的性能数据使用余弦相似度法、欧氏距离法进行相似度评价和一致性判别。

## 1 实验方法

### 1.1 粉体数据

采用中国科学院理化技术研究所和齐鲁中科光物理与工程技术研究院在廊坊园区共建的燃烧合成氮化硅粉体中试基地生产的氮化硅粉体为原料,采集2022年3月17日至11月14日期间生产的Y系列粉体,共33批次粉体,批次号为Y220317~Y221114,每批次200 kg粉体,均化处理后随机抽取1 kg进行指标测量。各批号样品按日期顺序标记为0~32号,详细性能数据表见表S1。

### 1.2 粉体指标选取

所选取的粉体静态理化指标如表1所示。

采用Freeman FT4粉末流变仪(Freeman Technology, Malvern, UK)测试表征粉体的动态流动性,该测试设备是一种叶片混合式粉末流动测试仪<sup>[11]</sup>,广泛用于表征剪切应变条件下颗粒的流动状态,能够获得粉体的流动性、流动稳定性、压缩性、黏附性和团聚性,以及粉体对流速的敏感度,粉末处于松散堆积状态下的流动性质,在低应力均匀堆积状态时的松装密度和颗粒形状及颗粒间作用力大小<sup>[12-14]</sup>。测量的动态流动性指标如表2所示。

### 1.3 指标标准化变换

为了消除指标之间的量纲影响,使粉体性能的各指标之间具有可比性,须对数据进行去量纲化和归一处理,本研究采用线性归一化方法,将各指标参数值限定在[0, 1]之间:

$$x' = \frac{x - \min(x)}{\max(x) - \min(x)} \quad (1)$$

表1 氮化硅粉体产品理化指标体系及测量方法

Table 1 Physical and chemical index system and measurement methods for silicon nitride powder products

| General indicator  | Secondary indicator   | Symbol      | Unit              | Method  | Test equipment  |
|--------------------|-----------------------|-------------|-------------------|---|---|
| Physical property  | Particle size         | $D_{10}$    | μm                |   |   |
|                    |                       | $D_{50}$    | μm                | Laser diffraction method                        | Particle diameter sizer (Dandong Bettersize Instruments, Bettersiza 2600)             |
|                    |                       | $D_{90}$    | μm                |   |   |
| Component property | Bulk density          | $\rho_B$    | kg/m <sup>3</sup> | Weight-volume method                            | Intelligent integrated powder characterizer (Dandong Bettersize Instruments, BT-1001) |
|                    | Specific surface area | $S$         | m <sup>2</sup> /g | Gas adsorption method                           | Gas absorption powder specific surface tester (MicrotracBEL, Belsorp max II)          |
|                    | α phase content       | $A$         | % (in mass)       | Mean-normalised-intensity method                | X-ray diffractometers (Rigaku Corporation, MiniFlex600)                               |
| Moisture content   | O content             | O           | % (in mass)       | Infrared detection method (CO/CO <sub>2</sub> ) | Nitrogen/oxygen analyz (HORIBA, EMGA-820)   |
|                    | H <sub>2</sub> O      | % (in mass) |                   | Gravimetric method                              | Rapid moisture tester (Shenzhen Guanya, SZ-GY820FT)                                   |

表2 氮化硅粉体产品流动性指标体系及测量方法

Table 2 Fluidity index system and measurement method of silicon nitride powder products

| General indicator                | Secondary indicator             | Symbol           | Unit   | Definition  |
|----------------------------------|---------------------------------|------------------|--------|---|
| Stability and variable flow rate | Basic flowability energy        | BFE              | mJ     | The energy required for the rotor to overcome the resistance of the powder to rotate  |
|                                  | Stability index                 | SI               | —      | Repeated measurements of powder flow energy to characterise its stability   |
|                                  | Flow rate index                 | FRI              | —      | Measurement of flow energy at different speeds  |
| Compressibility                  | Specific energy                 | SE               | mJ/g   | Data measured during the upward movement of the blade through the powder sample   |
|                                  | Conditioned bulk density        | CBD              | g/mL   | Loose packing density of pre-treated powders  |
|                                  | Compressibility                 | CPS <sub>m</sub> | %      | Compressibility at positive stress $m$ kPa  |
| Shear test                       | Cohesion                        | C <sub>m</sub>   | kPa    | Shear strength at zero positive stress for a pre-consolidated positive stress of $m$ kPa  |
|                                  | Unconfined yield strength       | UYS <sub>m</sub> | kPa    | The maximum principal stress corresponding to a molar circle tangent to the yield trajectory at a pre-consolidation stress of $m$ kPa and a minimum principal stress of 0 |
|                                  | Maximum principal stress        | MPS <sub>m</sub> | kPa    | Maximum compressive stress calculated from the molar circle at steady state flow under a pre-consolidated positive stress of $m$ kPa                                      |
|                                  | Flow function                   | FF <sub>m</sub>  | —      | Ratio of the above maximum principal stress to the unconfined yield strength  |
|                                  | Angle of internal friction      | AIF              | °      | The angle between the shear linear yield trajectory and the $x$ -axis, characterizing the ease with which the powder particles can slide against each other               |
| Aeration test                    | Aerated energy                  | AE <sub>n</sub>  | —      | The energy required to move the powder sample when filling the gas at a rate of $n$ mm/s  |
|                                  | Aeration ratio                  | AR               | —      | Ratio of the base flow energy to the filling energy after the powder having reached stability in the filling test   |
|                                  | Normalized aeration sensitivity | NAS              | s/mm   | Sensitivity to the effect of air introduced by the powder, normalized BFE to air velocity ratio   |
| Permeability                     | Pressure drop                   | PD <sub>m</sub>  | 100 Pa | Pressure reduction after passing air through a powder sample when a positive stress of $m$ kPa is applied and the air velocity is maintained at 0.5 mm/s                  |

式中,  $x'$  是归一化后的数据,  $x$  是测量数据。

## 1.4 一致性评价方法

### 1.4.1 余弦相似度法

表征粉体性能的指标经过标准化变换后, 形成  $n$  个无量纲指标, 将此作为一个  $n$  维空间的向量, 余弦相似度法就是通过计算两个向量间夹角的余弦值来评估它们的相似度。基于余弦值的相似度评价判断依据为两个向量是否大致指向相同的方向, 当两个向量趋向相同的指向时, 余弦相似度的值趋近 1, 代表两种粉体的指标越相似; 当两个向量夹角趋向于  $90^\circ$  时, 余弦相似度趋近于 0, 代表两种粉体的差异越大。两个样品  $X$  和  $Y$  之间的余弦相似度  $S(X, Y)$  按照公式(2)进行计算。

$$S(X, Y) = \frac{\sum_{i=1}^n X_i Y_i}{\sqrt{\sum_{i=1}^n X_i^2} \sqrt{\sum_{i=1}^n Y_i^2}} \quad (2)$$

式中,  $X$  为一个样品的特性指标测量数值组对应标准化处理值组构成的向量;  $Y$  为另一个样品的特性指标测量数值组对应标准化处理值组构成的向量。 $n$  为粉体特性指标的个数。 $X_i$  为向量  $X$  的第  $i$  个分量即第  $i$  个标准化处理值;  $Y_i$  为向量  $Y$  的第  $i$  个分量即第  $i$  个标准化处理值。

### 1.4.2 欧氏距离法

欧氏距离计算的是  $n$  维空间中两点之间的真实距离, 基于欧氏距离的相似度来判定个体的相似程度, 距离越近就越相似。两个样品  $X$  和  $Y$  之间的欧氏距离  $d(X, Y)$  按照公式(3)进行计算。

$$d(X, Y) = \sqrt{\sum_{i=1}^n (X_i - Y_i)^2} \quad (3)$$

式中各参数的意义同式(2)。

若基于欧氏距离, 将不同批次粉体分为  $M$  个类  $\omega_1 \omega_2 \dots \omega_{m_0}$ , 每个类中有  $N_i$  个样品,  $\omega_i$  类表示  $X^{(\omega_i)} = (x_1^{(\omega_i)}, x_2^{(\omega_i)}, \dots, x_{N_i}^{(\omega_i)})^T$ 。对任意待识别(分类)样品  $X = (x_1, x_2, \dots, x_n)$ , 计算

$$d^2(X, \omega_i) = |x - \overline{x^{(\omega_i)}}|^2 \quad (4)$$

其中,  $\overline{x^{(\omega_i)}}$  表示第  $i$  类的中心, 比较  $x$  到各类中心的距离, 若满足  $d(x, x_i^{(\omega_i)}) < d(X, \overline{x^{(\omega_j)}})$ ,  $j=1, 2, 3, \dots, M, i \neq j$ , 则  $X \in \omega_i$ 。

## 2 结果与讨论

### 2.1 关键指标分析

所有批次的氮化硅粉体测量全部理化指标和流动性指标, 所测量的粉体性能原始数据列在表 S1 中。每个样品有共计 23 项指标, 其中氧含量、 $\alpha$  相含量和粒度三个指标为衡量粉体品质的关键指标。低氧含量的氮化硅粉体有利于制备高热导率的制品<sup>[15]</sup>, 高  $\alpha$  相含量的氮化硅粉体在烧结过程中能够通过  $\alpha \rightarrow \beta$  相溶解析出机制, 形成晶粒互锁结构, 从而获得高强度高韧性的氮化硅陶瓷<sup>[16]</sup>。粒径分布决定粉体的烧结活性, 进而影响陶瓷制品的品质。

燃烧合成法制备的 Y220317~Y221102 系列氮化硅粉体的粒度、氧含量分布和  $\alpha$  相含量分布情况如图 1 所示。粒径分布  $D_{10}, D_{50}, D_{90}$  均在较窄范围内, 且更集中分布在细粒度范围内。本研究收集的是经过燃烧合成获得的原粉粒径, 而陶瓷烧结使用的亚微米粉体还需经历研磨细化等后处理步骤。原粉粒径的分布波动范围小, 对后处理阶段的工艺稳定有利。氧的含量在 0.678%~1.699%(质量分数)范围内波动, 中位数低于 0.9%, 属于低氧含量粉体。较高氧含量(>1%)粉体集中在早期 3 月 17 日至 4 月 15 日期间生产的 6 批次粉体中, 随着技术进步, 氧含量可控制在 1% 以下。 $\alpha$  相的含量分布在 88%~95.5%(质量分数)之间, 中位数高于 93%, 粉体整体呈现高  $\alpha$  相含量的特征。

### 2.2 余弦相似度评价

将 Y220317~Y221102 批次粉体理化指标和流动性指标数据按照 1.3 节所述的方法进行归一化, 随后按照 1.4.1 节所述的余弦相似度计算方法计算每两个批次间的余弦相似度, 计算所得余弦相似度数据表见表 S2, 所获得相似度数据绘制成热力图如图 2 所示。

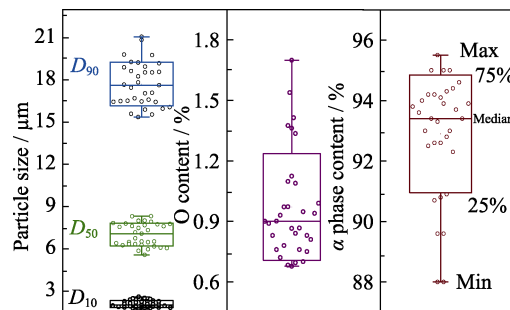


图 1 粒度、氧含量和  $\alpha$  相含量分布箱线图

Fig. 1 Box plots of particle size, oxygen content and  $\alpha$  phase content distribution

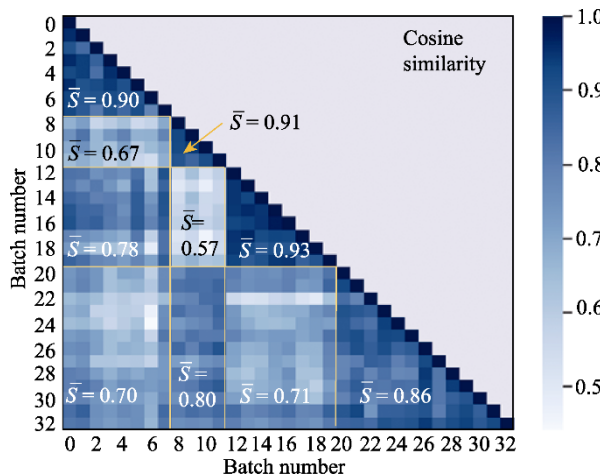


图 2 不同批次氮化硅粉体的余弦相似度热力图  
Fig. 2 Heat map of cosine similarity of different batches of silicon nitride powders

在余弦相似度热力图中根据颜色深浅划分为如图 2 所示的 10 个区域, 每个区域内标注的数值为该区域中相似度的平均值。由图 2 可知, 粉体在四个连续时间段内呈现高度相似的特征, 分别为批次 0~7(Y220317~Y220415), 批次 8~11(Y220503~Y220606), 批次 12~19(Y220629~Y220830) 和批次 20~32(Y220907~Y221114), 四组粉体组内的批次相似度的平均值分别为 0.90, 0.91, 0.93 和 0.86。在此四个时间段内粉体性质近似, 一致性较好。四个时间段互相间的相似度高低不一, 批次 8~11 与批次 20~32 两组粉体之间相似度的平均值为 0.80, 批次 0~7 与批次 12~19 两组粉体之间相似度的平均值为 0.78, 相似度较高, 性质可能相似, 但是批次 8~11 与批次 12~19 间的相似度仅为 0.57, 表示粉体间存在较大差异。

在氮化硅粉体的生产过程中, 工艺参数与产品质量属性之间的关系较复杂, 使控制产品质量的关键工艺参数难以分辨。上述余弦相似度计算结果说明几个时间段内的生产工艺参数可能发生变化, 造成粉体产品的一致性降低。因此, 对四个时间段内的生产条件进行排查调研, 重点对原材料、制备工艺和工艺参数的差异进行对比分析, 结果发现, 这四个时间段内的原料硅粉分别属于硅粉厂家不同批次的产品, 粒径分布相似但颗粒的微观形貌存在差异, 而原料硅粉的形貌差异导致了不同的氮化硅粉体性质。由余弦相似度分析结合生产条件可以确定, 控制原料硅粉性能的稳定是稳定控制氮化硅粉体性能的关键因素之一。此方法为进一步控制氮化硅粉体的生产工艺提供依据, 使生产过程更加明确且可控。

### 2.3 欧式距离聚类分析

对 Y220317~Y221102 批次粉体理化指标和流

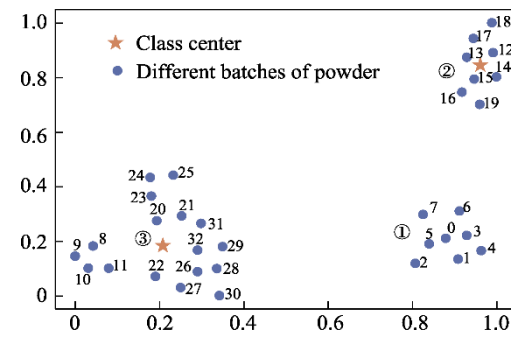


图 3 t-SNE 法可视化粉体的性能指标

Fig. 3 Performance indicators for the visualization of powders by the t-SNE method

动性指标数据按照 1.3 节所述的方法进行归一化处理, 随后按照 1.4.2 节所述的欧式距离计算方法计算每两个批次间的欧式距离。由于高维空间的欧式距离无法直观进行聚类判断, 因此对样品数据进行降维处理, 本研究采用 t-SNE(t-distribution Stochastic Neighbor Embedding)算法<sup>[17]</sup>将数据集映射至二维空间, 如图 3 所示。

图 3 中每个点分别代表一个样品, 样品间的距离越近则二者越相似。通过将距离接近的样品归为一类可将所有批次样品聚类成为 3 个类, 类 1 为批次 0~7, 类 2 为批次 12~19, 类 3 为批次 8~11 和批次 20~30。此三个类别对照余弦相似度的计算结果, 对应  $S > 0.8$  条件下的分类。余弦相似度最低的两组, 即批次 8~11 和批次 12~19 在图 3 中位于距离最远的对角线位置, 这表明欧式距离法和余弦相似度法均可实现粉体相似度的量化显示, 且计算结果相近, 两种评价方式能够相互验证。

使用 1.4.2 节中的方法计算每个类的类中心, 以五星形状标记在图 3 中。此类中心可以作为每个类别的粉体性能的特征指标, 类中心的参数如表 3 所示。类中心指标可用于后续新生产粉体的分类判断。对新生产粉体, 对比其到三个类中心的欧式距离, 将其划分入距离最短的一类。经过分类, 每一类粉体性质的一致性提高, 有利于保证粉体的批次稳定性。

## 3 结论和展望

本研究针对燃烧合成氮化硅粉体的一致性评价问题, 构建了以静态理化指标、动态流动性指标为主的粉体性能参数体系, 测试获得氮化硅粉体在该参数体系下的数据后, 使用余弦相似度法、欧式距离法进行一致性评价, 结果表明:

- 1) 使用该参数体系计算的余弦相似度和欧式

表3 三个类中心处粉体性能指标  
Table 3 Performance index of powder at three class centers

| General indicator                | Secondary indicator             | Symbol                   | Unit        | Class ①           | Class ② | Class ③ |
|----------------------------------|---------------------------------|--------------------------|-------------|-------------------|---------|---------|
| Physical/chemical indicator      | Physical property               | $D_{10}$                 | μm          | 1.870             | 1.854   | 2.275   |
|                                  |                                 | $D_{50}$                 | μm          | 6.439             | 6.158   | 7.798   |
|                                  |                                 | $D_{90}$                 | μm          | 16.819            | 16.038  | 19.092  |
|                                  | Component property              | Bulk density             | $\rho_B$    | kg/m <sup>3</sup> | 0.229   | 0.211   |
|                                  |                                 | Specific surface area    | $S$         | m <sup>2</sup> /g | 2.599   | 2.480   |
|                                  |                                 | $\alpha$ phase content   | $A$         | % (in mass)       | 92.625  | 94.350  |
| Stability and variable flow rate | O content                       | O                        | % (in mass) | 1.368             | 0.940   | 0.800   |
|                                  | Moisture content                | H <sub>2</sub> O         | % (in mass) | 1.086             | 1.206   | 1.654   |
|                                  |                                 | Basic flowability energy | BFE         | mJ                | 412.750 | 458.000 |
| Compressibility                  | Stability index                 | SI                       | —           | 1.058             | 1.009   | 1.033   |
|                                  | Flow rate index                 | FRI                      | —           | 1.840             | 1.659   | 1.731   |
|                                  | Specific energy                 | SE                       | mJ/g        | 9.283             | 8.986   | 9.423   |
| Liquidity indicator              | Conditioned bulk density        | CBD                      | g/mL        | 0.295             | 0.287   | 0.403   |
|                                  | Compressibility                 | CPS <sub>m</sub>         | %           | 32.463            | 37.462  | 33.388  |
|                                  | Cohesion                        | C <sub>m</sub>           | kPa         | 1.609             | 1.949   | 1.711   |
| Shear test                       | Unconfined yield strength       | UYS <sub>m</sub>         | kPa         | 6.540             | 7.874   | 6.989   |
|                                  | Maximum principal stress        | MPS <sub>m</sub>         | kPa         | 28.175            | 28.337  | 28.281  |
|                                  | Flow function                   | FF <sub>m</sub>          | —           | 4.341             | 3.619   | 4.055   |
| Aeration Test                    | Angle of internal friction      | AIF                      | °           | 37.612            | 37.325  | 37.800  |
|                                  | Aerated energy                  | AE <sub>n</sub>          | —           | 100.200           | 140.750 | 104.262 |
|                                  | Aeration ratio                  | AR                       | —           | 4.053             | 3.975   | 6.719   |
| Permeability                     | Normalized aeration sensitivity | NAS                      | s/mm        | 0.119             | 0.089   | 0.119   |
|                                  | Pressure drop                   | PD <sub>m</sub>          | mbar        | 20.025            | 12.492  | 5.169   |

距离均能反映批次粉体间的相似程度，两种评价方式的计算结果相互验证；

2) 对余弦相似度法一致性评价中判定为存在差异的粉体，结合生产工艺的变化，找到了控制氮化硅粉体性能稳定的关键因素(原料硅粉)；

3) 使用欧氏距离法对氮化硅粉体进行聚类分析，实现了粉体组别划分，以类中心和类间距为判断为新生产粉体批次划分提供了量化依据。

所建立氮化硅粉体评价指标体系为控制氮化硅粉体生产的批次稳定性提供了有效手段和量化依据。

但对于粉体性能一致性评价问题，仍处于起步阶段，尚存在以下不足，相应工作仍需完善。(1)当前研究对粉体的分类是基于粉体指标数据的聚类分析，未结合应用粉体后制品的性能。而在实际应用中，使用粉体制备的制品性能更受关注。在已获得的粉体分类基础上，进行制品性能评价，对分类结果进行进一步优化，合并制品性能相近的类别，最终获得在应用场景中批次稳定的粉体的指标范围。(2)当前研究中获得的批次划分结果还存在不同批次中指标相近的情况，原因是数据规模偏小。当数据量扩展之后，可以使用深度学习等自适应的机

器学习方法，通过自监督学习方式挖掘指标之间的相关性，使粉体性能体系中的指标获得精简完善，更好地完成粉体性能一致性评价任务。

#### 补充材料：

与本文相关补充材料可以登录 <https://doi.org/10.15541/jim20230058> 查阅。

#### 参考文献：

- [1] KATZ R N. High-temperature structural ceramics. *Science*, 1980, **208**(23): 841.
- [2] RILEY F L. Silicon nitride and related materials. *Journal of the American Ceramic Society*, 2000, **83**(2): 245.
- [3] WANG L, HE G, WU X M, et al. Effect of Si particle size and NH<sub>4</sub>Cl additive on combustion synthesis of α-Si<sub>3</sub>N<sub>4</sub>. *Ceramics International*, 2019, **45**(17): 21635.
- [4] WANG L, HE G, YANG Z, et al. Combustion synthesis of α-Si<sub>3</sub>N<sub>4</sub> powders using *in-situ* nano-SiO<sub>2</sub> coated Si and Si<sub>3</sub>N<sub>4</sub> reactants. *Ceramics International*, 2021, **47**(4).
- [5] 朱宇璇, 智强, 王波, 等. α-Si<sub>3</sub>N<sub>4</sub>粉体原料对多孔氮化硅陶瓷微观组织和力学性能的影响. 硅酸盐学报, 2019, **47**(9): 1254.
- [6] 于琦, 马越, 徐梅, 等. 氮化硅原料对陶瓷球性能的影响. 轴承, 2019(5): 23.
- [7] 周兰, 李兆军. 颗粒标准体系研究. 中国标准化, 2019(S1): 144.

- [8] 赵洁, 瞿海斌, 田埂, 等. 基于粉体学性质的流化床制粒质量一致性评价方法. 浙江大学学报(工学版), 2020, **54(2)**: 374.
- [9] 张孝娜, 孙会敏, 王珏, 等. 羧甲基纤维素钠质量一致性评价及性能参数智能可视化研究. 药学学报, 2020, **55(8)**: 1923.
- [10] 张煜皓, 王雅雯, 宿军慧, 等. 中药粉体物理指纹图谱研究进展. 分析测试学报, 2021, **40(1)**: 139.
- [11] FREEMAN R. Measuring the flow properties of consolidated, conditioned and aerated powders — a comparative study using a powder rheometer and a rotational shear cell. *Powder Technology*, 2007, **174(1/2)**: 25.
- [12] HARE C, ZAFAR U, GHADIRI M, et al. Analysis of the dynamics of the FT4 powder rheometer. *Powder Technology*, 2015, **285**: 123.
- [13] FORTE G, CLARK P J, YAN Z, et al. Using a freeman FT4 rheometer and electrical capacitance tomography to assess powder blending. *Powder Technology*, 2018, **337**: 25.
- [14] NAN W, GHADIRI M, WANG Y. Analysis of powder rheometry of FT4: effect of air flow. *Chemical Engineering Science*, 2017, **162**: 141.
- [15] ZHOU Y, HYUGA H, KUSANO D, et al. A tough silicon nitride ceramic with high thermal conductivity. *Advanced Materials*, 2011, **23(39)**: 4563.
- [16] SHEN Z, ZHAO Z, PENG H, et al. Formation of tough interlocking microstructures in silicon nitride ceramics by dynamic ripening. *Nature*, 2002, **417(16)**: 266.
- [17] VAN DER MAATEN L, HINTON G. Visualizing data using t-SNE. *Journal of Machine Learning Research*, 2008, **9**: 2579.

补充材料:

# 燃烧合成氮化硅粉体的性能一致性评价方法和应用

李宏华<sup>1</sup>, 东婉茹<sup>2</sup>, 王良<sup>1</sup>, 杨增朝<sup>1</sup>, 李江涛<sup>1</sup>

(1. 中国科学院 理化技术研究所, 低温重点实验室, 北京 100190; 2. 齐鲁中科光物理与工程研究院, 济南 250000)

**表 S1 原粉测量数据**

| 批号 | 测试时间     | 相含量        |      | 粒度/ $\mu\text{m}$ |          | 氧含量   | 水分    | 松堆密度<br>( $\text{g}\cdot\text{cm}^{-3}$ ) | 比表面<br>( $\text{m}^2\cdot\text{g}^{-1}$ ) | 稳定性和变流速 |     |       |      |      | 压缩性   |          |      | 剪切性能 |      |      | 充气性  |      |      | 透气性    |       |
|----|----------|------------|------|-------------------|----------|-------|-------|---|---|---------|-----|-------|------|------|-------|----------|------|------|------|------|------|------|------|--------|-------|
|    |          | %          |      | $D_{10}$          | $D_{50}$ |       |       |   |   | BFE     | SI  | FRI   | SE   | CBD  | CPS   | Cohesion | UYS  | MPS  | FF   | AIF  | AE   | AR   | NAS  | PD(压降) |       |
| 0  | Y220317  | 2022.3     | 93.9 | 1.864             | 6.57     | 17.1  | 1.362 | 1.46                                      | 0.24                                      | 2.590   | 413 | 1.07  | 1.82 | 9.25 | 0.291 | 33.1     | 1.64 | 6.63 | 28.1 | 4.24 | 37.2 | 105  | 3.98 | 0.119  | 22.7  |
| 1  | Y220321  | 2022.3     | 93.3 | 1.865             | 6.798    | 17.88 | 1.414 | 0.98                                      | 0.24                                      | 2.770   | 450 | 1.09  | 1.78 | 9.62 | 0.310 | 33.4     | 1.61 | 6.48 | 27.9 | 4.31 | 37.2 | 97.9 | 4.35 | 0.117  | 11.5  |
| 2  | Y2203172 | 2022.3     | 95.0 | 2.02              | 6.518    | 16.52 | 1.124 | 0.77                                      | 0.208                                     | 2.210   | 382 | 1.04  | 1.8  | 8.85 | 0.272 | 32.8     | 1.48 | 6.13 | 28.4 | 4.63 | 38.6 | 94.5 | 3.86 | 0.105  | 19.7  |
| 3  | Y2201141 | 2022.3     | 90.8 | 1.868             | 6.317    | 16.75 | 1.699 | 1.24                                      | 0.22                                      | 2.790   | 407 | 1.06  | 1.81 | 9.46 | 0.294 | 32.1     | 1.57 | 6.39 | 28   | 4.39 | 37.6 | 106  | 3.7  | 0.118  | 23.9  |
| 4  | Y2201142 | 2022/4/19  | 90.7 | 1.933             | 6.531    | 17.14 | 1.538 | 0.71                                      | 0.213                                     | 2.610   | 418 | 1.02  | 1.92 | 9.5  | 0.289 | 31       | 1.58 | 6.34 | 27.9 | 4.4  | 37.1 | 95.9 | 4.41 | 0.137  | 13.9  |
| 5  | Y2204022 | 2022/4/15  | 93.0 | 1.796             | 6.376    | 16.65 | 1.375 | 0.94                                      | 0.23                                      | 2.790   | 375 | 1.03  | 1.86 | 9.03 | 0.28  | 32.7     | 1.71 | 6.97 | 28.8 | 4.12 | 37.8 | 95.3 | 3.82 | 0.111  | 23.2  |
| 6  | Y2204021 | 2022/4/15  | 93.4 | 1.707             | 6.019    | 15.94 | 1.336 | 1.07                                      | 0.24                                      | 2.510   | 365 | 1.1   | 1.93 | 9.04 | 0.292 | 31       | 1.37 | 5.58 | 27.8 | 4.99 | 37.7 | 76   | 4.8  | 0.144  | 21.1  |
| 7  | Y220415  | 2022/4/15  | 90.9 | 1.907             | 6.387    | 16.57 | 1.098 | 1.52                                      | 0.24                                      | 2.520   | 492 | 1.05  | 1.8  | 9.51 | 0.336 | 33.6     | 1.91 | 7.8  | 28.5 | 3.65 | 37.7 | 131  | 3.5  | 0.103  | 24.2  |
| 8  | Y220503  | 2022/5/4   | 88.0 | 2.496             | 7.73     | 18.58 | 0.678 | 1.65                                      | 0.268                                     | 1.720   | 474 | 1.11  | 1.83 | 9.26 | 0.355 | 32.6     | 1.68 | 6.71 | 27.7 | 4.13 | 36.7 | 99.6 | 5.04 | 0.0736 | 2.45  |
| 9  | Y220513  | 2022/5/19  | 88.0 | 2.239             | 7.127    | 17.5  | 0.865 | 1.14                                      | 0.246                                     | 2.040   | 482 | 1.07  | 1.86 | 9.7  | 0.337 | 30.2     | 1.59 | 6.41 | 28.1 | 4.23 | 37.3 | 111  | 4.5  | 0.0743 | 1.19  |
| 10 | Y220602  | 2022/6/2   | 89.6 | 2.378             | 7.522    | 17.68 | 0.683 | 0.84                                      | 0.266                                     | 1.620   | 495 | 1.06  | 1.85 | 9.64 | 0.355 | 29.1     | 1.55 | 6.28 | 28   | 4.45 | 37.4 | 81.4 | 7.09 | 0.0955 | 4.1   |
| 11 | Y220606  | 2022/6/6   | 89.6 | 2.58              | 7.97     | 18.31 | 0.695 | 1.03                                      | 0.254                                     | 1.750   | 531 | 1     | 1.68 | 9.03 | 0.351 | 31.5     | 1.61 | 6.55 | 27.7 | 4.22 | 37.6 | 95.7 | 5.82 | 0.0896 | 5.87  |
| 12 | Y220629  | 2022/6/29  | 93.7 | 1.793             | 6.212    | 16.48 | 1.089 | 1.15                                      | 0.20                                      | 2.540   | 508 | 1     | 1.67 | 9.31 | 0.294 | 37.9     | 2.02 | 8.17 | 28.5 | 3.48 | 37.5 | 152  | 3.76 | 0.0965 | 11.7  |
| 13 | Y220630  | 2022/6/30  | 94.1 | 1.836             | 6.294    | 16.55 | 0.972 | 0.89                                      | 0.204                                     | 2.470   | 440 | 1.01  | 1.62 | 8.69 | 0.284 | 37.5     | 1.95 | 7.99 | 28.6 | 3.58 | 37.9 | 130  | 3.56 | 0.0634 | 14.7  |
| 14 | Y220715  | 2022/7/15  | 93.0 | 1.779             | 5.617    | 15.42 | 0.841 | 0.84                                      | 0.228                                     | 2.720   | 451 | 1     | 1.76 | 9.12 | 0.298 | 38.1     | 1.86 | 7.56 | 28.3 | 3.75 | 37.6 | 135  | 3.87 | 0.0963 | 11.9  |
| 15 | Y220726  | 2022/7/28  | 94.2 | 1.831             | 5.906    | 15.59 | 0.971 | 1.07                                      | 0.213                                     | 2.36    | 453 | 1.03  | 1.64 | 8.82 | 0.285 | 35.7     | 1.84 | 7.46 | 28   | 3.76 | 37.4 | 115  | 4.25 | 0.0881 | 14.5  |
| 16 | Y220727  | 2022/7/28  | 95.5 | 1.873             | 6.131    | 16.00 | 0.867 | 1.19                                      | 0.214                                     | 2.44    | 424 | 1.02  | 1.73 | 8.88 | 0.291 | 37.3     | 1.78 | 7.17 | 28.1 | 3.91 | 37.2 | 132  | 4.21 | 0.103  | 14.8  |
| 17 | Y220808  | 2022/8/10  | 94.3 | 1.946             | 6.571    | 16.5  | 0.931 | 1.13                                      | 0.196                                     | 2.71    | 424 | 0.987 | 1.64 | 8.75 | 0.272 | 37.1     | 2.05 | 8.26 | 28.6 | 3.47 | 37.1 | 133  | 3.96 | 0.0814 | 9.44  |
| 18 | Y220816  | 2022/8/16  | 95   | 1.952             | 6.444    | 16.12 | 0.948 | 1.71                                      | 0.216                                     | 2.53    | 484 | 0.995 | 1.58 | 8.97 | 0.282 | 38.7     | 2.3  | 9.16 | 28.6 | 3.12 | 36.7 | 187  | 3.82 | 0.0844 | 11.7  |
| 19 | Y220830  | 2022/8/30  | 95   | 1.819             | 6.091    | 15.64 | 0.902 | 1.67                                      | 0.219                                     | 2.07    | 480 | 1.03  | 1.63 | 9.35 | 0.291 | 37.4     | 1.79 | 7.22 | 28   | 3.88 | 37.2 | 142  | 4.37 | 0.102  | 11.2  |
| 20 | Y220907  | 2022/9/7   | 94.2 | 2.175             | 7.215    | 17.71 | 0.780 | 1.17                                      | 0.229                                     | 1.880   | 471 | 0.968 | 1.8  | 9.54 | 0.308 | 33.8     | 1.75 | 7.09 | 28.4 | 4    | 37.5 | 110  | 6.74 | 0.0579 | 0.735 |
| 21 | Y220921  | 2022/9/21  | 94.4 | 2.264             | 7.661    | 18.58 | 0.830 | 1.29                                      | 0.274                                     | 1.75    | 517 | 1.05  | 1.75 | 9.54 | 0.346 | 40       | 1.67 | 6.89 | 28.4 | 4.12 | 38.2 | 161  | 4.44 | 0.0827 | 1.19  |
| 22 | Y220923  | 2022/9/26  | 92.6 | 2.416             | 8.054    | 19    | 0.760 | 2.69                                      | 0.256                                     | 1.96    | 509 | 0.995 | 1.74 | 9.59 | 0.341 | 29.7     | 1.53 | 6.34 | 28.3 | 4.46 | 38.6 | 48.5 | 14.9 | 0.0839 | 2.95  |
| 23 | Y220927  | 2022/9/27  | 92.6 | 2.383             | 8.046    | 19.29 | 0.720 | 2.57                                      | 0.256                                     | 1.77    | 531 | 0.986 | 1.68 | 9.75 | 0.343 | 34.7     | 1.92 | 7.77 | 28.4 | 3.65 | 37.3 | 94.7 | 5.34 | 0.0873 | 3.81  |
| 24 | Y220928  | 2022/9/28  | 92.8 | 2.468             | 8.37     | 19.82 | 0.700 | 1.69                                      | 0.259                                     | 1.87    | 562 | 0.944 | 1.67 | 9.74 | 0.351 | 31.5     | 2    | 8.23 | 29.6 | 3.59 | 38   | 122  | 5.45 | 0.114  | 7.1   |
| 25 | Y220930  | 2022/9/30  | 94   | 2.308             | 7.787    | 18.68 | 0.760 | 2.61                                      | 0.246                                     | 1.81    | 600 | 1.07  | 1.74 | 10   | 0.351 | 34.8     | 1.82 | 7.66 | 29.4 | 3.84 | 39.1 | 139  | 4.83 | 0.105  | 5.5   |
| 26 | Y221026  | 2022/10/26 | 92.5 | 2.25              | 7.838    | 19.33 | 0.750 | 1.73                                      | 0.263                                     | 1.73    | 497 | 1.03  | 1.7  | 9.13 | 0.332 | 36.2     | 1.72 | 7.02 | 28   | 3.99 | 37.8 | 76.3 | 8.57 | 0.151  | 6.42  |
| 27 | Y221027  | 2022/10/28 | 93.4 | 2.071             | 7.371    | 18.62 | 0.830 | 1.97                                      | 0.26                                      | 1.97    | 534 | 1.05  | 1.51 | 9.57 | 0.345 | 35.5     | 1.81 | 7.39 | 28   | 3.78 | 37.7 | 40.3 | 15.8 | 0.14   | 8.3   |
| 28 | Y221103  | 2022/11/2  | 93.6 | 2.127             | 7.65     | 19.24 | 0.810 | 1.86                                      | 0.288                                     | 1.86    | 435 | 1.02  | 1.75 | 8.92 | 0.315 | 33.9     | 1.62 | 6.51 | 27.7 | 4.25 | 37.2 | 109  | 5.01 | 0.182  | 6.73  |
| 29 | Y221104  | 2022/11/4  | 93.9 | 2.26              | 8.356    | 21.13 | 0.89  | 1.01                                      | 0.281                                     | 2.16    | 471 | 1.04  | 1.75 | 9.13 | 0.321 | 32.3     | 1.56 | 6.47 | 28.2 | 4.35 | 38.4 | 109  | 5.3  | 0.173  | 6.6   |
| 30 | Y221107  | 2022/11/9  | 92.3 | 2.05              | 7.604    | 18.95 | 0.94  | 1.21                                      | 0.257                                     | 1.94    | 490 | 1.04  | 1.74 | 9.13 | 1.335 | 35.1     | 1.68 | 6.9  | 28.3 | 4.1  | 38.1 | 97.1 | 6.53 | 0.161  | 7.18  |
| 31 | Y221109  | 2022/11/9  | 94.6 | 2.082             | 7.814    | 19.86 | 0.9   | 1.05                                      | 0.258                                     | 2.13    | 547 | 1.05  | 1.73 | 9.44 | 0.34  | 33.9     | 1.77 | 7.16 | 28.3 | 3.95 | 37.3 | 184  | 3.31 | 0.134  | 7.59  |
| 32 | Y221114  | 2022/11/15 | 93.8 | 2.021             | 7.874    | 20.9  | 0.99  | 2.13                                      | 0.245                                     | 2.19    | 493 | 1.02  | 1.72 | 9.2  | 0.328 | 33.2     | 1.84 | 7.54 | 28.4 | 3.77 | 38.1 | 99.6 | 5.57 | 0.159  | 5.73  |

表 S2 余弦相似度计算数据结果

|    | 0     | 1     | 2     | 3     | 4         | 5     | 6     | 7     | 8     | 9     | 10    | 11    | 12    | 13    | 14    | 15    | 16    | 17    | 18    | 19    | 20    | 21    | 22    | 23    | 24    | 25    | 26    | 27    | 28    | 29    | 30    | 31    | 32    |
|----|-------|-------|-------|-------|-----------|-------|-------|-------|-------|-------|-------|-------|-------|-------|-------|-------|-------|-------|-------|-------|-------|-------|-------|-------|-------|-------|-------|-------|-------|-------|-------|-------|-------|
| 0  | 1     | 0.957 | 0.9   | 0.96  | 0.922     | 0.957 | 0.93  | 0.927 | 0.677 | 0.749 | 0.695 | 0.651 | 0.827 | 0.81  | 0.853 | 0.892 | 0.904 | 0.786 | 0.736 | 0.86  | 0.741 | 0.747 | 0.654 | 0.683 | 0.65  | 0.728 | 0.758 | 0.716 | 0.798 | 0.796 | 0.768 | 0.832 | 0.814 |
| 1  | 0.957 | 1     | 0.843 | 0.937 | 0.938     | 0.9   | 0.89  | 0.883 | 0.718 | 0.822 | 0.75  | 0.686 | 0.82  | 0.765 | 0.835 | 0.847 | 0.854 | 0.758 | 0.697 | 0.836 | 0.774 | 0.786 | 0.676 | 0.699 | 0.66  | 0.742 | 0.769 | 0.746 | 0.788 | 0.827 | 0.788 | 0.865 | 0.824 |
| 2  | 0.9   | 0.843 | 1     | 0.864 | 0.834     | 0.915 | 0.9   | 0.81  | 0.569 | 0.665 | 0.664 | 0.648 | 0.75  | 0.812 | 0.795 | 0.847 | 0.865 | 0.735 | 0.62  | 0.781 | 0.739 | 0.739 | 0.648 | 0.582 | 0.619 | 0.711 | 0.716 | 0.624 | 0.722 | 0.792 | 0.742 | 0.758 | 0.748 |
| 3  | 0.96  | 0.937 | 0.864 | 1     | 0.955     | 0.943 | 0.916 | 0.9   | 0.6   | 0.732 | 0.637 | 0.585 | 0.778 | 0.742 | 0.8   | 0.816 | 0.809 | 0.708 | 0.639 | 0.765 | 0.643 | 0.644 | 0.586 | 0.576 | 0.563 | 0.648 | 0.648 | 0.621 | 0.676 | 0.713 | 0.695 | 0.737 | 0.725 |
| 4  | 0.922 | 0.938 | 0.834 | 0.955 | 1         | 0.906 | 0.897 | 0.848 | 0.641 | 0.791 | 0.716 | 0.636 | 0.752 | 0.676 | 0.778 | 0.758 | 0.78  | 0.684 | 0.596 | 0.724 | 0.709 | 0.662 | 0.606 | 0.595 | 0.599 | 0.637 | 0.678 | 0.61  | 0.715 | 0.758 | 0.722 | 0.771 | 0.744 |
| 5  | 0.957 | 0.9   | 0.915 | 0.943 | 0.906     | 1     | 0.898 | 0.914 | 0.554 | 0.677 | 0.607 | 0.567 | 0.83  | 0.849 | 0.875 | 0.874 | 0.881 | 0.816 | 0.722 | 0.783 | 0.702 | 0.674 | 0.582 | 0.59  | 0.635 | 0.675 | 0.669 | 0.618 | 0.694 | 0.741 | 0.718 | 0.757 | 0.759 |
| 6  | 0.93  | 0.89  | 0.9   | 0.916 | 0.897     | 0.898 | 1     | 0.785 | 0.581 | 0.681 | 0.657 | 0.542 | 0.636 | 0.641 | 0.733 | 0.763 | 0.787 | 0.587 | 0.489 | 0.712 | 0.592 | 0.613 | 0.571 | 0.47  | 0.442 | 0.571 | 0.643 | 0.582 | 0.723 | 0.726 | 0.688 | 0.682 | 0.67  |
| 7  | 0.927 | 0.883 | 0.81  | 0.9   | 0.848     | 0.914 | 0.785 | 1     | 0.695 | 0.785 | 0.703 | 0.684 | 0.902 | 0.858 | 0.898 | 0.896 | 0.876 | 0.826 | 0.826 | 0.874 | 0.768 | 0.773 | 0.653 | 0.758 | 0.763 | 0.818 | 0.758 | 0.732 | 0.73  | 0.747 | 0.767 | 0.844 | 0.817 |
| 8  | 0.677 | 0.718 | 0.569 | 0.6   | 0.641     | 0.554 | 0.581 | 0.695 | 1     | 0.926 | 0.922 | 0.897 | 0.546 | 0.503 | 0.547 | 0.568 | 0.587 | 0.514 | 0.532 | 0.634 | 0.769 | 0.827 | 0.772 | 0.832 | 0.73  | 0.778 | 0.846 | 0.723 | 0.811 | 0.796 | 0.754 | 0.804 | 0.76  |
| 9  | 0.749 | 0.822 | 0.665 | 0.732 | 0.791     | 0.677 | 0.681 | 0.785 | 0.926 | 1     | 0.947 | 0.856 | 0.643 | 0.557 | 0.651 | 0.614 | 0.629 | 0.558 | 0.543 | 0.674 | 0.829 | 0.835 | 0.786 | 0.801 | 0.764 | 0.827 | 0.791 | 0.694 | 0.754 | 0.808 | 0.766 | 0.837 | 0.77  |
| 10 | 0.695 | 0.75  | 0.664 | 0.637 | 0.716     | 0.607 | 0.657 | 0.703 | 0.922 | 0.947 | 1     | 0.914 | 0.538 | 0.476 | 0.556 | 0.553 | 0.576 | 0.46  | 0.447 | 0.622 | 0.827 | 0.831 | 0.835 | 0.802 | 0.783 | 0.806 | 0.848 | 0.749 | 0.806 | 0.853 | 0.792 | 0.822 | 0.762 |
| 11 | 0.651 | 0.686 | 0.648 | 0.585 | 0.636     | 0.567 | 0.542 | 0.684 | 0.897 | 0.856 | 0.914 | 1     | 0.588 | 0.567 | 0.567 | 0.6   | 0.609 | 0.559 | 0.551 | 0.638 | 0.824 | 0.855 | 0.841 | 0.856 | 0.841 | 0.81  | 0.897 | 0.772 | 0.834 | 0.881 | 0.807 | 0.846 | 0.81  |
| 12 | 0.827 | 0.82  | 0.75  | 0.778 | 0.752     | 0.83  | 0.636 | 0.902 | 0.546 | 0.643 | 0.538 | 0.588 | 1     | 0.949 | 0.949 | 0.946 | 0.929 | 0.951 | 0.947 | 0.932 | 0.8   | 0.786 | 0.556 | 0.733 | 0.742 | 0.787 | 0.71  | 0.704 | 0.654 | 0.675 | 0.717 | 0.838 | 0.796 |
| 13 | 0.81  | 0.765 | 0.812 | 0.742 | 0.676     | 0.849 | 0.641 | 0.858 | 0.503 | 0.557 | 0.476 | 0.567 | 0.949 | 1     | 0.929 | 0.959 | 0.935 | 0.964 | 0.921 | 0.878 | 0.752 | 0.757 | 0.519 | 0.657 | 0.687 | 0.729 | 0.676 | 0.648 | 0.62  | 0.665 | 0.685 | 0.779 | 0.751 |
| 14 | 0.853 | 0.835 | 0.795 | 0.8   | 0.778     | 0.875 | 0.733 | 0.898 | 0.547 | 0.651 | 0.556 | 0.567 | 0.949 | 0.929 | 1     | 0.948 | 0.951 | 0.917 | 0.882 | 0.903 | 0.766 | 0.77  | 0.526 | 0.647 | 0.654 | 0.714 | 0.684 | 0.652 | 0.67  | 0.678 | 0.707 | 0.794 | 0.735 |
| 15 | 0.892 | 0.847 | 0.847 | 0.816 | 0.758     | 0.874 | 0.763 | 0.896 | 0.568 | 0.614 | 0.553 | 0.6   | 0.946 | 0.959 | 0.948 | 1     | 0.979 | 0.931 | 0.907 | 0.945 | 0.755 | 0.769 | 0.558 | 0.67  | 0.65  | 0.731 | 0.724 | 0.714 | 0.705 | 0.698 | 0.722 | 0.814 | 0.77  |
| 16 | 0.904 | 0.854 | 0.865 | 0.809 | 0.78      | 0.881 | 0.787 | 0.876 | 0.587 | 0.629 | 0.576 | 0.609 | 0.929 | 0.935 | 0.951 | 0.979 | 1     | 0.929 | 0.89  | 0.948 | 0.791 | 0.794 | 0.578 | 0.687 | 0.659 | 0.731 | 0.748 | 0.699 | 0.757 | 0.732 | 0.74  | 0.835 | 0.787 |
| 17 | 0.786 | 0.758 | 0.735 | 0.708 | 0.684     | 0.816 | 0.587 | 0.826 | 0.514 | 0.558 | 0.46  | 0.559 | 0.951 | 0.964 | 0.917 | 0.931 | 0.929 | 1     | 0.959 | 0.866 | 0.767 | 0.725 | 0.519 | 0.69  | 0.706 | 0.702 | 0.672 | 0.645 | 0.635 | 0.65  | 0.663 | 0.781 | 0.764 |
| 18 | 0.736 | 0.697 | 0.62  | 0.639 | 0.596     | 0.722 | 0.489 | 0.826 | 0.532 | 0.543 | 0.447 | 0.551 | 0.947 | 0.921 | 0.882 | 0.907 | 0.89  | 0.959 | 1     | 0.897 | 0.747 | 0.734 | 0.495 | 0.739 | 0.726 | 0.726 | 0.671 | 0.667 | 0.634 | 0.596 | 0.637 | 0.788 | 0.746 |
| 19 | 0.86  | 0.836 | 0.781 | 0.765 | 0.724     | 0.783 | 0.712 | 0.874 | 0.634 | 0.674 | 0.622 | 0.638 | 0.932 | 0.878 | 0.903 | 0.945 | 0.948 | 0.866 | 0.897 | 1     | 0.822 | 0.852 | 0.638 | 0.781 | 0.714 | 0.825 | 0.788 | 0.781 | 0.767 | 0.718 | 0.753 | 0.864 | 0.808 |
| 20 | 0.741 | 0.774 | 0.739 | 0.643 | 0.709     | 0.702 | 0.592 | 0.768 | 0.769 | 0.829 | 0.827 | 0.824 | 0.8   | 0.752 | 0.766 | 0.755 | 0.791 | 0.767 | 0.747 | 0.822 | 1     | 0.925 | 0.838 | 0.901 | 0.888 | 0.893 | 0.852 | 0.781 | 0.782 | 0.824 | 0.789 | 0.887 | 0.852 |
| 21 | 0.747 | 0.786 | 0.739 | 0.644 | 0.662     | 0.674 | 0.613 | 0.773 | 0.827 | 0.835 | 0.831 | 0.855 | 0.786 | 0.757 | 0.77  | 0.769 | 0.794 | 0.725 | 0.734 | 0.852 | 0.925 | 1     | 0.785 | 0.885 | 0.845 | 0.912 | 0.906 | 0.801 | 0.85  | 0.875 | 0.847 | 0.927 | 0.862 |
| 22 | 0.654 | 0.676 | 0.648 | 0.586 | 0.606     | 0.582 | 0.571 | 0.653 | 0.772 | 0.786 | 0.835 | 0.841 | 0.556 | 0.519 | 0.526 | 0.558 | 0.578 | 0.519 | 0.495 | 0.638 | 0.838 | 0.785 | 1     | 0.869 | 0.824 | 0.857 | 0.871 | 0.869 | 0.782 | 0.82  | 0.763 | 0.739 | 0.84  |
| 23 | 0.683 | 0.699 | 0.582 | 0.576 | 0.595     | 0.59  | 0.47  | 0.758 | 0.832 | 0.801 | 0.802 | 0.856 | 0.733 | 0.657 | 0.647 | 0.67  | 0.687 | 0.69  | 0.739 | 0.781 | 0.901 | 0.885 | 0.869 | 1     | 0.936 | 0.928 | 0.909 | 0.857 | 0.83  | 0.814 | 0.792 | 0.865 | 0.901 |
| 24 | 0.65  | 0.66  | 0.619 | 0.563 | 0.599     | 0.635 | 0.442 | 0.763 | 0.73  | 0.764 | 0.783 | 0.841 | 0.742 | 0.687 | 0.654 | 0.65  | 0.659 | 0.706 | 0.726 | 0.714 | 0.888 | 0.845 | 0.824 | 0.936 | 1     | 0.92  | 0.86  | 0.796 | 0.774 | 0.834 | 0.792 | 0.869 | 0.887 |
| 25 | 0.728 | 0.742 | 0.711 | 0.648 | 0.637     | 0.675 | 0.571 | 0.818 | 0.778 | 0.827 | 0.806 | 0.81  | 0.787 | 0.729 | 0.714 | 0.731 | 0.731 | 0.702 | 0.726 | 0.825 | 0.893 | 0.912 | 0.857 | 0.928 | 0.92  | 1     | 0.88  | 0.832 | 0.782 | 0.828 | 0.82  | 0.879 | 0.9   |
| 26 | 0.758 | 0.769 | 0.716 | 0.648 | 0.678     | 0.669 | 0.643 | 0.758 | 0.846 | 0.791 | 0.848 | 0.897 | 0.71  | 0.676 | 0.684 | 0.724 | 0.748 | 0.672 | 0.671 | 0.788 | 0.852 | 0.906 | 0.871 | 0.909 | 0.86  | 0.88  | 1     | 0.922 | 0.945 | 0.936 | 0.899 | 0.896 | 0.941 |
| 27 | 0.716 | 0.746 | 0.624 | 0.621 | 0.61      | 0.618 | 0.582 | 0.732 | 0.723 | 0.694 | 0.749 | 0.772 | 0.704 | 0.648 | 0.652 | 0.714 | 0.699 | 0.645 | 0.667 | 0.781 | 0.781 | 0.801 | 0.869 | 0.857 | 0.796 | 0.832 | 0.922 | 1     | 0.819 | 0.814 | 0.815 | 0.8   | 0.872 |
| 28 | 0.798 | 0.788 | 0.722 | 0.676 | 0.715     | 0.694 | 0.723 | 0.73  | 0.811 | 0.754 | 0.806 | 0.834 | 0.654 | 0.62  | 0.67  | 0.705 | 0.757 | 0.635 | 0.634 | 0.767 | 0.782 | 0.85  | 0.782 | 0.83  | 0.774 | 0.782 | 0.945 | 0.819 | 1     | 0.941 | 0.867 | 0.893 | 0.913 |
| 29 | 0.796 | 0.827 | 0.792 | 0.713 | 0.758     | 0.741 | 0.726 | 0.747 | 0.796 | 0.808 | 0.853 | 0.881 | 0.675 | 0.665 | 0.678 | 0.698 | 0.732 | 0.65  | 0.596 | 0.718 | 0.824 | 0.875 | 0.82  | 0.814 | 0.834 | 0.828 | 0.936 | 0.814 | 0.941 | 1     | 0.893 | 0.923 | 0.934 |
| 30 | 0.768 | 0.788 | 0.742 | 0.695 | 0.722     | 0.718 | 0.688 | 0.767 | 0.754 | 0.766 | 0.792 | 0.807 | 0.717 | 0.685 | 0.707 | 0.722 | 0.74  | 0.663 | 0.637 | 0.753 | 0.789 | 0.847 | 0.763 | 0.792 | 0.82  | 0.899 | 0.815 | 0.867 | 0.893 | 1     | 0.867 | 0.883 |       |
| 31 | 0.832 | 0.865 | 0.758 | 0.737 | 0.771</td |       |       |       |       |       |       |       |       |       |       |       |       |       |       |       |       |       |       |       |       |       |       |       |       |       |       |       |       |